

Phase Behavior and Polymer/Solvent Interactions in Thermoreversible Gels of Syndiotactic Poly(methyl methacrylate)[†]

Alberto Saiani,[‡] Jiří Spěváček,[§] and Jean-Michel Guenet^{*,‡}

Laboratoire de Dynamique des Fluides Complexes,[‡] Université Louis Pasteur-UMR 7506, 4, rue Blaise Pascal, F-67070 Strasbourg Cedex, France, and Institute of Macromolecular Chemistry, Academy of Sciences of the Czech Republic, Heyrovsky Square 2, CZ-16206 Prague 6, Czech Republic

Received July 17, 1997; Revised Manuscript Received November 4, 1997

ABSTRACT: The temperature–concentration phase diagrams have been established for sPMMA gels prepared from toluene, chlorobenzene, and bromobenzene. In these three solvents polymer–solvent compounds are formed: one compound in toluene (two toluene molecules/three monomers) and two compounds in bromobenzene and chlorobenzene (two solvent molecules/three monomers and three solvent molecules/two monomers). In addition, in chlorobenzene the existence of a mesophase above the macroscopic gel melting is shown. Neutron diffraction and NMR investigations give further support to the existence of these compounds. NMR measurements of selective and nonselective ¹H spin–lattice relaxation rates R_1 of the solvent are consistent with the stoichiometry derived from the phase diagrams and also indicate that the mobility of the solvent in the sPMMA/bromobenzene compounds is quite high.

Introduction

The mechanisms whereby solutions of stereoregular polymers are turned into thermoreversible gels have aroused growing interest these past few years.¹ Originally, thermoreversible gelation, which consists in mutual chains aggregation, was thought to arise from a *liquid–liquid* phase separation, i.e., involving poor solvents.² Evidence was gradually gathered, however, showing that this phenomenon can also occur in good solvents.^{3–5} Under these conditions gelation takes place through a *liquid–solid* phase separation instead.⁵ Clearly, the quality of the solvent in the sense developed by Flory for amorphous polymers⁶ is not the keystone to thermoreversible gelation. In fact, experimental arguments have been provided for systems such as those involving polystyrenes (isotactic or syndiotactic) that the solvent promotes chain stiffening, which eventually produces gels instead of chain-folded crystals.^{7–9} This stiffening process is said to be achieved by the intercalation of solvent molecules into the cavities created by the phenyl groups, which results in the stabilization of a given helical conformation of the chains.^{8,10} This stabilization effect is indirectly suggested by the existence of polymer–solvent compounds as is deduced from the temperature–concentration phase diagrams.¹¹

The involvement of the solvent is also believed to contribute in the gelation process of syndiotactic poly(methyl methacrylate).^{4,12,13} Although the gelation and aggregation of this polymer have received considerable attention this past decade, the part played by the solvent remains to be clarified. The purpose of this paper is an attempt to cast some light on this topic by combining three different approaches: determination of the temperature–concentration phase diagrams whose

outcomes will be examined in the light of neutron diffraction and NMR results.

Experimental Section

1. Materials. The three highly-syndiotactic sPMMA samples used in this study were synthesized in toluene at –78 °C by ion-coordination polymerization with triethylaluminum and titanium (IV) chloride as catalysts.¹⁴ Two were protonated samples (sPMMA1 and sPMMA2) and one (sPMMA3) was deuterated (monomer purchased from Eurisotop, Saclay, France). For the sake of comparison for the NMR spectroscopy investigation, a PMMA sample of lower degree of stereoregularity (at-PMMA) was prepared by radical polymerization in acetic acid at 30 °C with dibenzoyl peroxide as initiator in the presence of RhCl(C₆H₁₂)(4-methylpyridine).

Molecular weight characterization was performed by means of SEC in THF at 25 °C using the universal calibration method. The following values were obtained: sPMMA1, $M_w = 1.0 \times 10^5$ with $M_w/M_n = 1.8$; sPMMA2, $M_w = 1.35 \times 10^5$ with $M_w/M_n = 1.4$; sPMMA3, $M_w = 1.52 \times 10^5$ with $M_w/M_n = 1.44$. The less syndiotactic sample was characterized by osmometry measurements: at-PMMA, $M_n = 4.2 \times 10^4$.

The tacticity of the samples was determined in deuterated chloroform by means of proton NMR spectroscopy. The following values were found for the proportions of syndiotactic, heterotactic, and isotactic triads, respectively: sPMMA1 and sPMMA2, S = 89%; H = 9%; I = 2%. at-PMMA, S = 66%; H = 31%; I = 3%.

2. Sample Preparation. a. DSC Samples. Two procedures were used for producing adequate DSC samples.

The first procedure was used for concentrations lower than 45% (w/w). Homogeneous solutions were prepared by heating in hermetically closed testtubes a mixture of polymer and solvent at a temperature close to the solvent boiling point. Gels were formed by a subsequent quench of these solutions at 4 °C. Pieces of gel were then transferred into “volatile sample” DSC pans that were hermetically sealed.

The second procedure was employed for concentrations higher than 45% (w/w) as preparation of gels as described above, although achievable, was found to be time-consuming. Here, the samples were prepared by allowing evaporation of the solvent from low-concentrated solutions (typically 35% w/w) until the desired concentration was reached as monitored by sample weighing. The samples were then introduced into the DSC pans, hermetically sealed, and subsequently heated

* To whom correspondence should be addressed.

[†] This work has been supported by a grant from the EEC (Human Capital and Mobility Programme) enabling the creation of a laboratories network entitled “Polymer–solvent organization in relation to chain microstructure”.

[‡] Université Louis Pasteur.

[§] Academy of Sciences of the Czech Republic.

until homogeneous systems were obtained. Forty-five and 50% samples were also prepared by the first procedure in order to test the reliability of the second procedure. No significant discrepancy was observed between either type of sample. The size of the symbols used in the phase diagrams is representative of the uncertainty on the determination of the endotherm maximum.

b. Neutron Diffraction Samples. The gels were prepared directly in amorphous silica tubes (3-mm inner diameter). After introducing a mixture of polymer and solvent these tubes were sealed hermetically from atmosphere. Homogeneous solutions were prepared by heating this mixture close to the solvent boiling point and were then rapidly quenched to 4 °C for achieving gelation. The gels were aged 2 weeks at 4 °C and 25 °C prior to the neutron diffraction study.

c. NMR Samples. Homogeneous solutions of sPMMA2 in bromobenzene ($C = 4.5\text{--}27.4$ wt %) and toluene- d_6 ($C = 0.2\text{--}10$ wt %), as well as at-PMMA in bromobenzene ($C = 12.3$ wt %), were prepared by heating the sealed 5-mm NMR tubes at 90 °C. The solutions in bromobenzene, for which spin-lattice relaxation rates were also measured, were degassed at elevated temperature (above 70 °C) and sealed under argon. sPMMA gels were allowed to form at room temperature.

3. Techniques. a. Differential Scanning Calorimetry. Investigations were carried out by means of a DSC 30 apparatus from METTLER equipped with the TA4000 system for processing the raw data.

Prior to any measurements the gels were melted in the hermetically-sealed DSC pan. The samples prepared by evaporation were further annealed for 30 min at high temperature (close to solvent boiling point) so as to make them homogeneous. For all the systems the following temperature scans were used while recording the DSC traces: (i) cooling down to -30 °C to observe gelation; (ii) heating up close to solvent boiling point to detect the different thermal events; (iii) cooling down again to -100 °C to achieve solvent crystallization after gelation; (iv) heating up to determine the solvent melting point and the associated latent heat.

To assess the effect of the aging process upon the gel thermal behavior, samples were aged for a minimum of 2 weeks at either 4 or 25 °C after subsequent melting and quenching to -30 °C. The aged samples were then scanned from 4 or 25 °C up to a temperature close to solvent boiling point. In all cases several samples were prepared so as to explore the thermal behavior with heating and cooling rates ranging from 2 to 10 °C/m.

b. Neutron Diffraction. Neutron diffraction experiments were carried out on G-6-1, a diffraction camera located at Orphée (Laboratoire Léon Brillouin). G-6-1 is a two-axis spectrometer equipped with a banana-type BF_3 detector composed of 400 cells with an angular resolution of 0.2° . The spectrometer operates at a wavelength $\lambda = 0.474$ nm obtained by diffraction of the neutron beam onto a graphite monocrystal oriented under Bragg condition (further details available on request). Transfer momenta $q = (4\pi/\lambda) \sin(\theta/2)$ were ranging from $q = 2$ to 16 nm^{-1} . Detector normalization and correction for cell efficiency were achieved with the spectrum given off by a vanadium sample.

c. NMR. ^1H NMR spectra and ^1H spin-lattice relaxation rates R_1 were measured by using a Bruker AC-300 spectrometer operating at 300.1 MHz. The integrated intensities were determined by using the spectrometer's integration software with an accuracy to within $\pm 1\%$. The proton nonselective (NS) and selective (SE) R_1 values of the solvent were measured by using inversion recovery pulse sequence ($180^\circ - \tau - 90^\circ$) with eight scans separated by a relaxation delay of 60–100 s; 15–20 τ values were used. In selective $R_1(\text{SE})$ measurements the DANTE method¹⁵ was used to generate selectively the 180° pulse.¹⁶

Results and Discussion

Before presenting and discussing the results, the reason why chlorobenzene, bromobenzene, and toluene were selected for this study is worth clarifying. Recent

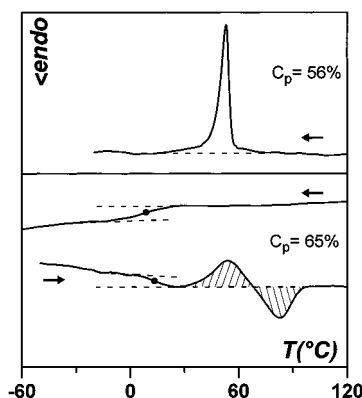


Figure 1. DSC traces of sPMMA2/chlorobenzene systems. Upper: exotherm observed on cooling a 56 wt % of solution. Lower: glass transition observed on cooling a 65 wt % solution and the resulting thermogramme obtained on heating.

investigations into the thermoreversible gelation of stereoregular polymers possessing side groups, such as polystyrenes, have highlighted the important role of the solvent in this phenomenon.¹ In particular, the adequacy between the shape and size of the solvent and the cavity created by the side groups when the chain takes on a given helical or near-helical structure has been recognized as a key factor.^{1,5,7,8} In the case of PMMA there is an additional effect due to the polarization of the ester function: the appearance of a negative fractional charge on the oxygen atom. Here the three solvents have been chosen because they possess approximately the same size (molar volume ranging from 102 to 106 cm^3/mol) but differ in their polarizability: a CH_3 group repels electrons while bromine or chlorine atoms attract them. If solvent molecules are effectively housed within sPMMA cavities, then it is likely that toluene will not be placed in the same way as chlorobenzene and/or bromobenzene. This difference should allow one to assess the solvent effect on the gelation habit of this polymer.

1. Thermal Analysis. Phase Diagrams. Generally speaking, the thermal behavior of the three systems under study can be broken down into three typical cases:

(i) For polymer concentrations lower than about 55–60%, a narrow gelation exotherm is observed on cooling (Figure 1). On reheating a broader melting endotherm is observed. The enthalpies associated with the exotherm and the corresponding endotherm are identical within experimental uncertainties (see Figure 2).

(ii) For polymer concentrations ranging from 60% to about 70% only the event due to the glass transition is recorded on cooling (see Figure 1). On reheating, an exotherm appears just after the occurrence of the glass transition and is immediately followed by a melting endotherm. Here, one observes a most unusual behavior: only the glass transition is seen on cooling as with slowly-crystallizing polymers while, as with rapidly-crystallizing polymers, "recrystallization" takes place just after passing through the glass transition. Again, the enthalpies associated with the exotherm and the endotherm are identical within experimental uncertainties.

(ii) For polymer concentrations above 70% only the glass transition is seen both on cooling and on heating.

As a rule, there exists a nonnegligible aging effect. As can be seen in Figure 2 the enthalpies associated with the melting events increase on an average by 20%. This increase turns out to be little dependent upon the

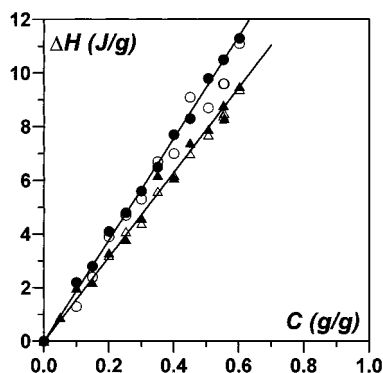


Figure 2. Formation and melting enthalpies for sPMMA2/toluene systems. Formation enthalpies (\blacktriangle); melting enthalpies measured immediately after gelation (\triangle); melting enthalpies after 2-week aging at 4 °C (\circ), melting enthalpies after 2-week aging at 25 °C (\bullet). Enthalpies are expressed in J/g of gel.

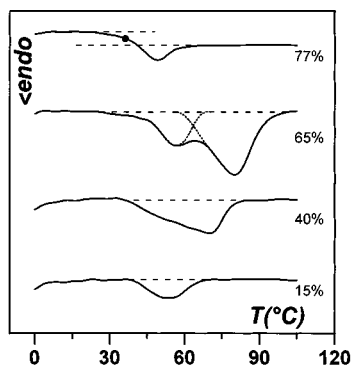


Figure 3. Typical DSC traces recorded in sPMMA2/toluene systems. Concentrations (wt) as indicated.

aging temperature for concentrations lower than 60%. In the present case aging at 4 or 25 °C gives virtually the same results (see Figure 2). Also, aging tends to improve the aspect and definition of the different endotherms, which is of invaluable help for establishing the temperature–concentration phase diagrams. The experimental results presented in what follows have been obtained after a 2-week aging at 25 °C.

Thermograms recorded on heating after subsequent aging differ slightly from one solvent to another as the temperature–concentration phase diagrams do:

(i) In **toluene** (see Figure 3), below 60% only one endotherm is seen. From 60% to 70% two endotherms appear: a minor endotherm (the low-melting endotherm) and a major endotherm (the high-melting endotherm). These two endotherms do not arise from any fusion–recrystallization effect as the thermogram aspect does not change with the heating rate nor do the associated enthalpies. Above, 70% only the glass transition can be seen.

The temperature–concentration phase diagram portrayed in Figure 4 suggests the formation of a congruently-melting polymer–solvent compound. This is ascertained by the evolution of the melting enthalpy which goes through a maximum at about 60%. From this maximum the stoichiometry of the compound can be derived and found to be approximately equal to *2 toluene molecules/3 monomers*. Above 60% the compound forms a eutectic with either a solid phase or another compound. This point cannot be further precised with the data at hand nor can the necessary information be gained on the melting behavior in the high concentra-

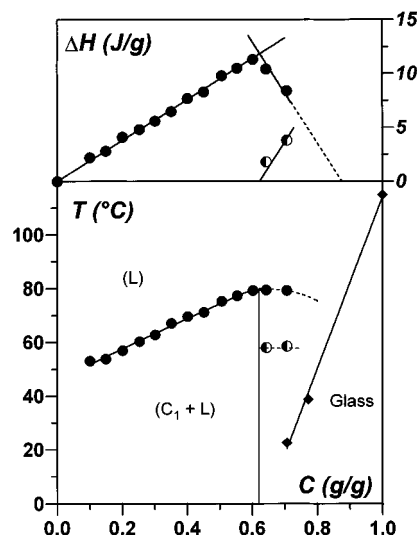


Figure 4. Temperature–concentration phase diagram and Tamman's diagram for sPMMA2/toluene systems (enthalpy is in J/g of gel).

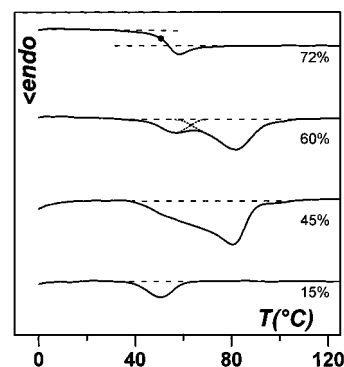


Figure 5. Typical DSC traces recorded in sPMMA/bromobenzene systems. Concentrations (wt) as indicated.

tion range due to the occurrence of the glass transition.

The existence of a polymer–solvent compound with sPMMA does not come as a surprise since it is known that the molecular organization of this polymer can only be achieved in the presence of solvent molecules.¹³

(ii) In **bromobenzene**, although all the DSC traces look quite similar to those given off by sPMMA/toluene systems (Figure 5), the phase diagram is slightly different (Figure 6). One fact compels to consider the occurrence of another event: *the variation of the melting enthalpy ΔH as a function of polymer concentration* departs significantly from linearity. This suggests that the measured enthalpy consists of two terms, which in turn implies that the melting endotherm is actually composed of two endotherms. The shape of ΔH vs C also suggests that one endotherm predominates at low polymer concentrations while the other gradually takes over at high polymer concentrations. Attempts to separate these supposed two endotherms by using very low heating rates failed.

After a realistic, judicious deconvolution procedure, the possible variations of the enthalpies of these two endotherms are shown in the T – C phase diagram of Figure 6. This results in postulating the existence of another compound (possibly with a singular point) whose stoichiometry is *3 bromobenzene molecules/2 monomers* (compound noted C_1). Thus, at a temperature of about 53 °C, the following reaction is likely to take place at the stoichiometric concentration:

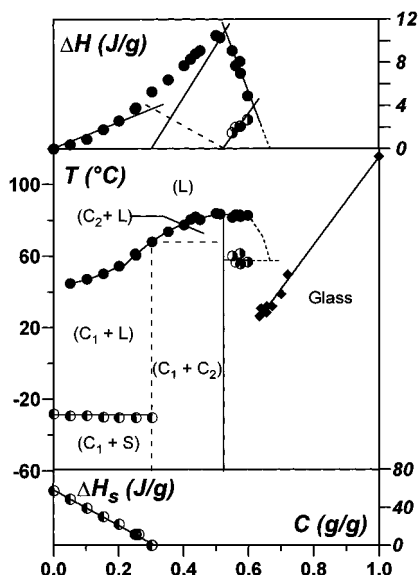
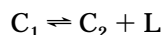


Figure 6. Temperature–concentration phase diagram and Tamman's diagram (upper, enthalpies associated with polymer melting; lower, enthalpies associated with solvent melting; all enthalpies are in J/g of gel) for sPMMA2/bromobenzene systems.



Here C_2 possesses a stoichiometry close to that of the sPMMA/toluene compound (here *1.9 bromobenzene molecules/3 monomers*). As is customary in a T – C phase diagram, the hypothetical nonvariant melting line of C_1 is dashed instead of solid.

The existence of the hypothetical compound C_1 receives additional support from the determination of the fraction of solvent molecules engaged in the polymer phase. This is achieved by studying the crystallization of the free solvent as a function of polymer concentration. As the fraction of free solvent decreases with increasing polymer concentration Gibbs phase rule indicates that the solvent melting enthalpy must decrease linearly. The polymer concentration at which this parameter becomes zero yields the number of solvent molecules “trapped” in the polymer phase. If the polymer phase is a compound, then this concentration corresponds to the stoichiometry. As can be seen this concentration equals within experimental uncertainties that derived for compound C_1 after the deconvolution procedure.

It is worth emphasizing that the study of the crystallization behavior of toluene was unsuccessful due to the irreproducibility of the results. This failure probably arises from the fact that toluene crystallizes at very low temperature (usually lower than -100 °C) where molecular mobility is strongly impeded.

(iii) In **chlorobenzene** an additional endotherm is distinctly seen after the main melting endotherm (Figures 7 and 8). Again, this endotherm does not originate in a fusion–recrystallization phenomenon as a variation of the heating rate does not alter its magnitude with respect to the main endotherm. After deconvolution the enthalpy of this second endotherm goes through a maximum at $C_{\text{pol}} \approx 0.47$ (w/w). The behavior of the melting enthalpy of the first endotherm first shows a linear variation in the range $C_{\text{pol}} = 0$ –35% (w/w), followed by a decrease and again a linear increase.

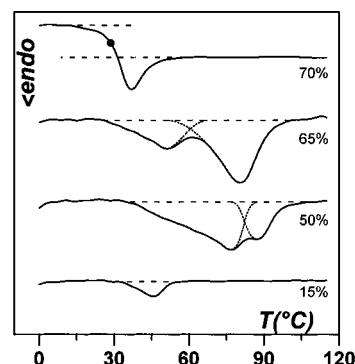


Figure 7. Typical DSC traces recorded in sPMMA2/chlorobenzene systems. Concentrations (wt) as indicated.

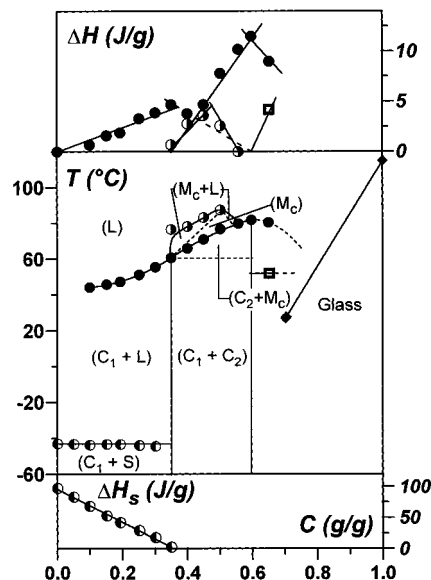


Figure 8. Temperature–concentration phase diagram and Tamman's diagram (upper, enthalpies associated with polymer melting; lower, enthalpies associated with solvent melting; all enthalpies are in J/g of gel) for sPMMA2/chlorobenzene systems.

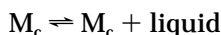
Here, it is quite conspicuous that the main endotherm is actually composed of two endotherms in the range 35–60% (w/w). As with bromobenzene, the compound is most probably characterized by a singular point (intermediate case between a congruently-melting compound and an incongruently-melting compound). The stoichiometry of this compound is *3.3 chlorobenzene molecules/2 monomers*, a value close to that found for sPMMA/bromobenzene.

As with bromobenzene, the existence of such a compound receives support from the crystallization behavior of the free solvent. The concentration at which free chlorobenzene molecules are no longer present does correspond to the stoichiometry of this compound.

Interestingly, the macroscopic melting of the system is completed at the onset of the second endotherm. At this temperature a mesophase, designated in what follows as M_c (possibly nematic-like), therefore occurs prior to the appearance of the isotropic liquid phase. The second endotherm corresponds to the transformation of this mesophase into the isotropic liquid phase. To summarize at the first endotherm the following transformation takes place:



while at the second endotherm one observes:



As the enthalpy of the second endotherm goes through a maximum it is likely that this mesophase is also constituted of a compound with a stoichiometry of nearly *0.85 chlorobenzene molecules/monomer*. Recent small-angle neutron scattering investigations¹⁷ have shown that, above the macroscopic melting of chlorobenzene/sPMMA systems, the chain still possesses a well-defined helical conformation, unlike what is seen in toluene or bromobenzene. The presence of this conformation may be responsible for the existence of this mesophase.

Bromobenzene and chlorobenzene exhibit very similar *T*-*C* phase diagrams, apart from the existence of a mesophase in the latter. In both solvents, two compounds are thought to occur instead of only one in toluene.

The validity of the existence of a compound possessing a higher degree of solvation in these two solvents can be further strengthened by a comparison of the melting temperatures in the three systems. In Figure 9 those temperatures are plotted as a function of the mole fraction of polymer which allows relevant comparison between the three systems. As can be seen, compound *C*₂ occurs virtually at the same mole fraction in the three systems (*f*_m ≈ 0.62), and its melting temperature is, within experimental uncertainties, independent of the solvent used. Similarly, from *f*_m ≈ 0.62 down to *f*_m ≈ 0.38–0.4, the latter corresponding to the stoichiometry of compound *C*₁, melting temperatures remain virtually independent of the solvent used. Conversely, for mole fractions lower than *f*_m ≈ 0.38, there appears a noticeable discrepancy between the melting temperatures in toluene, on the one hand, and those in bromobenzene and chlorobenzene, on the other hand. Melting in toluene occurs some 10 °C higher than in the two other solvents, a fact which can be simply accounted for in terms of degree of compound solvation. The less solvated compound (here *C*₂) must melt at a higher temperature than the more solvated compound¹⁸ (here *C*₁).

2. Neutron Diffraction. As has been shown in previous papers,²⁰ the existence of polymer–solvent compounds can be demonstrated qualitatively by using neutron diffraction together with the deuterium-labeled technique. The diffracted intensity is written:

$$I(q) \sim K_p S_p(q) + K_s S_s(q) + 2K_p K_s S_{ps}(q) \quad (1)$$

where *K* and *S*(*q*) with the appropriate subscripts are the contrast factor and the scattering function of the polymer, the solvent, and the cross-term between polymer and solvent. The cross-term *S*_{ps}(*q*) is only meaningful when polymer–solvent compounds are dealt with, which results in an alteration of the ratio of the diffracted intensities with respect with one another when different labeled species are used.^{19,20} Such is not the case in the absence of compound (“dry” crystallization). Thus, if significant variation of this ratio is observed when replacing one species by its labeled counterpart then polymer–solvent compounds are present beyond doubt.

Here we shall present only the qualitative aspect of the diffraction spectra with special attention on the first

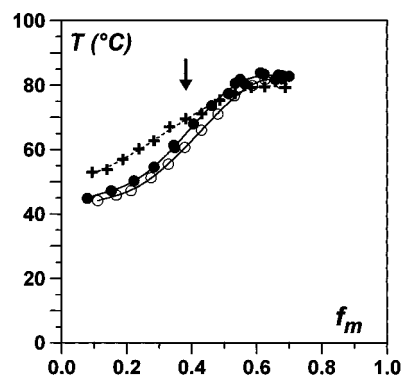


Figure 9. Macroscopic melting temperatures as a function of the polymer mole fraction for sPMMA2/toluene (+), sPMMA2/bromobenzene (●), and sPMMA2/chlorobenzene (○).

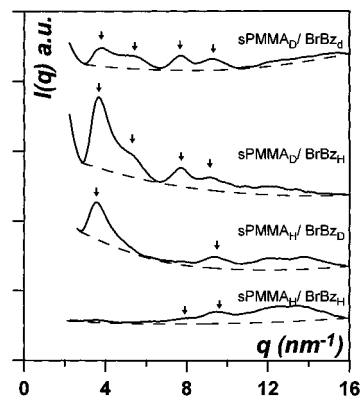


Figure 10. Neutron diffraction patterns for differing isotopic labelings (as indicated) of sPMMA/bromobenzene systems (*C* = 25 wt %) (sPMMA 1 and sPMMA D).

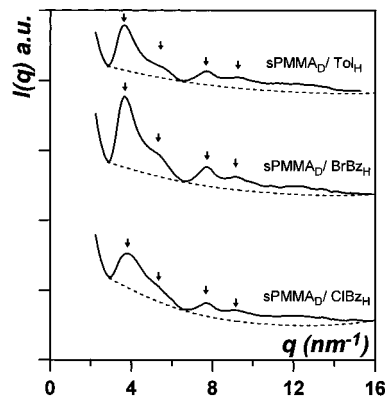


Figure 11. Neutron diffraction patterns for the same isotopic labeling (deuterated sPMMA/protonated solvent), *C* = 25 wt %.

four reflections. Detailed calculation as to the helical form involved will be postponed to a forthcoming paper. In Figures 10 and 11 are drawn the diffraction curves for 25% concentrated systems in bromobenzene with different labeled species and in the three solvents for the same labeling case (deuterated polymer with hydrogenous solvent).

Two results are worth emphasizing:

(i) The intensity ratio does vary when altering the labeling of the species. This is especially conspicuous between the first and the fourth reflections for which the ratio goes from about 1 to 4 when hydrogenous solvent is used in lieu of its deuterated counterpart.

(ii) Although the concentrations studied correspond to *C*₁ in bromobenzene and in chlorobenzene and to *C*₂

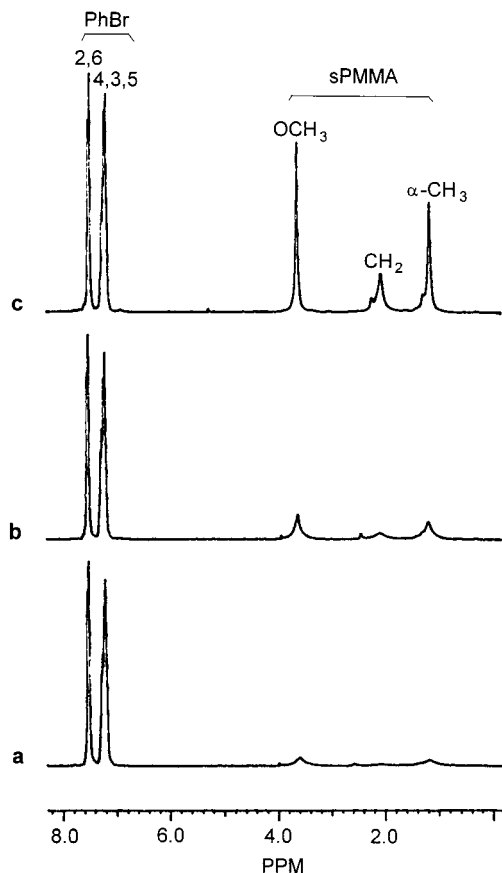


Figure 12. ^1H NMR spectra, 300.1 MHz, of sPMMA2 gel in bromobenzene ($C = 27.4$ wt %) at 25 °C (a), 40 °C (b), and 60 °C (c).

in toluene, no significant discrepancy is observed. This means that the structure is little dependent upon the degree of solvation.

3. NMR Spectroscopy. It has been shown in a number of papers that the physical association of polymers (including sPMMA) in solutions and gels can be conveniently followed by measuring the integrated intensities in high resolution ^1H NMR spectra.^{4,21} A sensitive method revealing the presence of associated structures and providing information on their thermal stability consists in determining the temperature dependence of integrated intensities of NMR lines. In Figure 12 the ^1H NMR spectra of sPMMA2 gel in bromobenzene ($C = 27.4$ wt %) obtained at three temperatures are shown. The lines of bromobenzene are in the left part, while the lines of sPMMA (toward higher field the lines of OCH_3 , CH_2 , and $\alpha\text{-CH}_3$ protons) are in the right part of these spectra. Spectra of Figure 12 show that at 25 and 40 °C most of sPMMA stands in the associated state with restricted mobility to such an extent as to escape detection in high-resolution ^1H NMR; this results in a marked reduction of the absolute integrated intensities of sPMMA in high-resolution spectra as the observed lines correspond only to the nonassociated units. At 60 °C a pronounced increase of the integrated intensities of all lines of sPMMA is clearly seen, which confirms the complete melting of the associated structures at this temperature. On the other hand, the measurements of the temperature dependences of the absolute integrated intensities of the ^1H NMR lines of bromobenzene in the range 25–110 °C (monotonously decreasing dependence with temperature) show that in the studied sPMMA gels all the

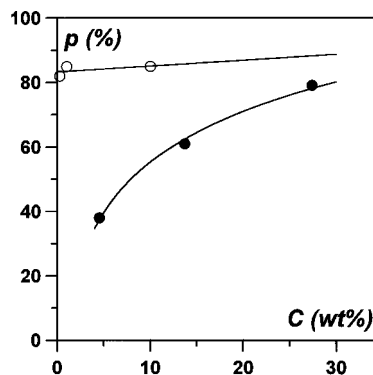


Figure 13. Associated polymer fraction as a function of polymer concentration for sPMMA2 in toluene- d_8 (○) and bromobenzene (●).

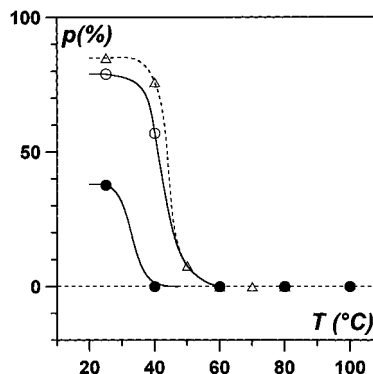


Figure 14. Temperature dependence of associated polymer fraction for sPMMA2 in toluene- d_8 ($C = 1$ wt %) (Δ) and in bromobenzene for $C = 4.5$ wt % (●) and $C = 27.4$ wt % (○).

solvent is detected in high-resolution spectra at room temperature; i.e., no “loss” of solvent intensity is observed even for 27.4 wt % gels (cf. Figure 12).

The fraction p of associated units of sPMMA can be determined by means of the following relation:^{4,21}

$$p = 1 - I/I_0 \quad (2)$$

where I and I_0 are the integrated intensities with and without association, respectively.

The value of I_0 was determined from solutions of sPMMA2 in CDCl_3 wherein no association occurs^{4,21} whatsoever. The values of associated fraction p are plotted as a function of polymer concentration for sPMMA2 systems in bromobenzene and in toluene- d_8 in Figure 13.

For sPMMA in toluene- d_8 the associated fraction p does not significantly depend upon polymer concentration in the range $C = 0.2$ –10 wt %, which is in agreement with the linear concentration dependence of the melting enthalpy ΔH observed in DSC measurements (Figures 2 and 4).

For sPMMA in bromobenzene the associated fraction p increases with increasing polymer concentration, evidently in connection with the significant departure of the concentration dependence of the melting enthalpy from linearity in this solvent (Figure 6). Also, the observed increase of the temperature of complete melting with polymer concentration as detected by ^1H NMR for sPMMA2 gels in bromobenzene (Figure 14) (40 °C for $C = 4.5$ wt %, 60 °C for $C = 27.4$ wt %) agrees well with DSC results (cf. Figure 6). In spite of a lower polymer concentration, the temperature of the complete melting of associated structures is about 10 °C higher

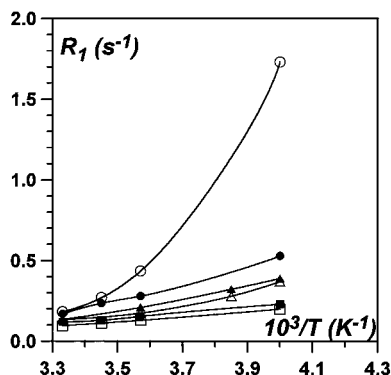


Figure 15. Selective (open symbols) and nonselective (filled symbols) proton spin-lattice relaxation rates of bromobenzene (2,6-protons) as a function of temperature in pure bromobenzene (squares), solution of at-PMMA ($C = 12.3$ wt %) (triangles) and sPMMA2 gel ($C = 13.7$ wt %) (circles) at 300.1 MHz.

for sPMMA2 in toluene- d_8 ($C = 1$ wt %) than for sPMMA2 in bromobenzene ($C = 4.5$ wt %). This again is in agreement with a lower degree of solvation of the polymer-solvent compound in toluene than in bromobenzene as is predicted by the phase diagrams.

In agreement with previous studies,⁴ no association was detected in solutions of at-PMMA in bromobenzene.

Recently, it has been shown that direct evidence for polymer/solvent complexes in thermoreversible gels can be obtained from the measurements of nonselective and selective proton spin-lattice relaxation rates R_1 of the solvent.¹⁶ Assuming a dipolar relaxation mechanism, for any proton i its nonselective, $R_1(\text{NS})$, and selective, $R_1(\text{SE})$, relaxation rates are given by:²²

$$R_1(\text{NS}) = \sum \rho_{ij} + \sum \sigma_{ij} \quad (3)$$

$$R_1(\text{SE}) = \sum \rho_{ij} \quad (4)$$

In these equations, ρ_{ij} and σ_{ij} are the direct relaxation term and the cross-relaxation term respectively for a pair of protons i and j :

$$\rho_{ij} = \frac{h^2 \gamma_H^4}{40\pi^2 r_{ij}^6} \times \left[\frac{3\tau_c}{1 + (\omega_0 \tau_c)^2} + \frac{6\tau_c}{1 + 4(\omega_0 \tau_c)^2} + \tau_c \right] \quad (5)$$

and

$$\sigma_{ij} = \frac{h^2 \gamma_H^4}{40\pi^2 r_{ij}^6} \times \left[\frac{6\tau_c}{1 + 4(\omega_0 \tau_c)^2} - \tau_c \right] \quad (6)$$

where r_{ij} is the interproton distance, ω_0 the resonance frequency, τ_c the motional correlation time, and other constants have their usual meanings. From eqs 3–6 it follows that relaxation rates $R_1(\text{NS})$ and $R_1(\text{SE})$ exhibit different dependence on the correlation time τ_c ; a marked difference exists in the slow-motion region, i.e., for correlation times $\tau_c > \omega_0^{-1}$. For the determination of the correlation time τ_c it is convenient to use the ratio $R_1(\text{NS})/R_1(\text{SE})$, where the interproton distance r_{ij} is eliminated; the limiting values for this ratio are 1.5 for $\omega_0 \tau_c \ll 1$ and 0 for $\omega_0 \tau_c \gg 1$.

The values of $R_1(\text{NS})$ and $R_1(\text{SE})$ of 2,6-protons (in *ortho* positions to Br) of bromobenzene in 13.7 wt % gel of sPMMA2 are plotted in Figure 15 as a function of temperature. $R_1(\text{NS})$ and $R_1(\text{SE})$ values for 2,6-protons

Table 1. Nonselective and Selective Proton Spin-Lattice Relaxation Rates and Correlation Times of Bromobenzene (PhBr) (2,6-Protons) in sPMMA Solutions and Gels

sample	T , °C	$R_1(\text{NS})$, ^a s^{-1}	$R_1(\text{SE})$, ^b s^{-1}	$R_1^{\text{B}}(\text{NS})/$ $R_1^{\text{B}}(\text{SE})$	τ_c , ns
PhBr	250	0.235	0.196		0.37
	300	0.125	0.102		0.34
at-PMMA $C = 12.3$ wt %	250	0.392	0.370		0.52
	300	0.139	0.123		0.45
sPMMA2 $C = 13.7$ wt %	250	0.526	1.724	0.155	3.1 ^b
	280	0.286	0.435	0.425	1.6 ^b
	300	0.168	0.189	0.64	1.1 ^b
sPMMA2 $C = 27.4$ wt %	300	0.333	0.465	0.68	1.05 ^b

^a Frequency 300.1 MHz; standard deviation less than 0.5%. ^b τ_c values of the bound bromobenzene.

of bromobenzene in pure solvent and in the solution of at-PMMA ($C = 12.3$ wt %) are also shown for the sake of comparison. While in the latter two cases $R_1(\text{SE})$ and $R_1(\text{NS})$ do not significantly differ, $R_1(\text{SE})$ being somewhat lower in comparison to $R_1(\text{NS})$ as expected for $\omega_0 \tau_c < 1$, a reverse situation exists with bromobenzene in sPMMA gels where $R_1(\text{SE}) > R_1(\text{NS})$. The difference between $R_1(\text{SE})$ and $R_1(\text{NS})$ in sPMMA gels increases with decreasing temperature. This result, together with the fact that $R_1(\text{NS})$ decreases with increasing temperature, shows that a part of bromobenzene molecules form a complex with sPMMA.¹⁶ That the relaxation curves in sPMMA gels are exponential (single R_1) indicates fast exchange between bound and free bromobenzene molecules; i.e., the lifetime of the complexed solvent molecules has to be ~ 100 ms or shorter. The observed spin-lattice relaxation rate R_1 is written for such a case:

$$R_1 = (1 - f)R_1^{\text{F}} + fR_1^{\text{B}} \quad (7)$$

where superscripts F and B correspond to the free state and to the bound state, respectively, and where f is the fraction of bound solvent molecules.

By using eq 7 the relaxation rates $R_1^{\text{B}}(\text{NS})$ and $R_1^{\text{B}}(\text{SE})$, and correspondingly the ratio $R_1^{\text{B}}(\text{NS})/R_1^{\text{B}}(\text{SE})$, have been calculated for bromobenzene in sPMMA2 gels ($C = 13.7$ wt % and $C = 27.4$ wt %) (see Table 1). The fraction f of bound solvent is given as

$$f = \frac{\alpha p C}{(1 - C)} \quad (8)$$

where α is the stoichiometric weight ratio (weight of the solvent/weight of sPMMA in the polymer-solvent complex), p is the associated polymer fraction, and C is the polymer concentration (polymer weight fraction). Based on DSC results (Figure 6), the C_1 polymer-solvent complex was assumed to contain 1.5 bromobenzene molecules per monomeric unit corresponding to $\alpha = 2.35$; this assumption is certainly correct for $C = 13.7$ wt %. The values of the associated polymer fraction p are shown in Figure 13. As no polymer-solvent complex occurs in at-PMMA/bromobenzene solutions, the values of R_1 as determined experimentally for this system (for $C = 12.3$ wt %) were taken for the values of R_1^{F} . These values undoubtedly correspond better to the behavior of free solvent in sPMMA gels than R_1 values for pure bromobenzene; at 300 K these values are

practically same as those for pure solvent (cf. Figure 15). The values of the ratio of relaxation rates of bound solvent $R_1^B(\text{NS})/R_1^B(\text{SE})$ for polymer concentrations of 13.7 and 27.4 wt % at 300 K are almost the same. The slight difference probably arises from the fact that for $C = 27.4$ wt % the polymer-solvent complex is not pure C_1 compound, but rather a mixture of C_1 and C_2 complexes (cf. the concentration dependence of melting enthalpy in Figure 6), and therefore for this concentration the effective value of α in eq 8 should be somewhat smaller than $\alpha = 2.35$.

From the ratio $R_1(\text{NS})/R_1(\text{SE})$ and by using eqs 3–6 the correlation times τ_c can be determined (see values in Table 1). For bromobenzene molecules in the pure state and in the at-PMMA solution, one derives $\tau_c \approx 0.35$ and 0.45 ns, respectively. For sPMMA gels the correlation time of bound solvent is $\tau_c = 1.1$ and 3.1 ns at 300 and 250 K, respectively (Table 1). The activation energy $\Delta E = 3.2$ kcal/mol as determined from the temperature dependence of the correlation time of bound bromobenzene in sPMMA gel ($C = 13.7$ wt %) is the same as the activation energy for bromobenzene in the solution of at-PMMA as determined from the temperature dependence of relaxation rates $R_1(\text{NS})$ and $R_1(\text{SE})$ ($\ln R_1$ vs T^{-1} plot). Although several times longer than that of the free solvent, the correlation time of the bound solvent is significantly shorter than the effective correlation time of the motion of associated segments of sPMMA, $\tau_{\text{eff}} \sim 70$ ns.^{23,24} This indicates relatively enough motional freedom for the complexed bromobenzene molecules which might be accommodated in cavities formed by side groups¹ as in the case of polystyrenes. A similar type of behavior was previously observed for substrate molecules interacting with enzyme.²²

This behavior is also preserved even in solid semicrystalline samples of sPMMA obtained from sPMMA gels by evaporation of the solvent at room temperature, where a part of solvent molecules (~ 15 mol %) remains bound; even here the molecules of the bound solvent retain relatively large anisotropic mobility.¹²

Concluding Remarks

Through the combination of three techniques (DSC, neutron diffraction, NMR), we have shown that sPMMA forms polymer-solvent complexes in the gel state. The number as well as the stoichiometry of these complexes is solvent-dependent. This, in our opinion, is linked to the placement of the solvent molecules on the helical structure. The results presented here suggest that this is in part related to the polarizability of the solvent.

Our results indicate that the stiff ordered conformation (probably a double helical form^{4,17,24}) of sPMMA in

the gel is at least partially stabilized by the solvent molecules; i.e., the solvent is not simply housed within the cavities created by the side-groups of an intrinsically-stable helix. That the mobility of the complexed solvent is higher than that of the segments belonging to the polymer does not necessarily imply that the helical form is intrinsically-stable. Indeed, decomplexation of a solvent molecule is most probably concomitant with the complexation of another one so that there is always a complexed solvent molecule at a given site of the helix.

Acknowledgment. J.S. gratefully acknowledges Grant 203/96/1386 of the Grant Agency of the Czech Republic.

References and Notes

- (1) Guenet, J.-M. *Thermoreversible Gelation of Polymers and Biopolymers*; Academic Press: London, 1992; Chapters 1 and 2.
- (2) Feke, G. T.; Prins, W. *Macromolecules* **1974**, *7*, 527.
- (3) Tan, H.; Hiltner, A.; Moet, E.; Baer, E. *Macromolecules* **1983**, *16*, 28. Gan, Y.; Nuffer, A.; Guenet, J. M.; François J. *Polym. Commun.* **1986**, *27*, 233.
- (4) Spěváček, J.; Schneider, B. *Adv. Colloid Interface Sci.* **1987**, *27*, 81.
- (5) Daniel, C.; Deluca, M. D.; Brulet, A.; Menelle, A.; Guenet, J. M. *Polymer* **1996**, *37*, 1273.
- (6) Flory, P. J. In *Principles of Polymer Chemistry*; Cornell University Press: Ithaca, NY, 1953.
- (7) Guenet, J. M. *Macromolecules* **1987**, *20*, 2874.
- (8) Klein, M.; Menelle, A.; Mathis, A.; Guenet, J. M. *Macromolecules* **1990**, *23*, 4591.
- (9) Guenet, J. M.; Menelle, A.; Schaffhauser, V.; Terech, P.; Thierry, A. *Colloid Polym. Sci.* **1994**, *272*, 36.
- (10) Guenet, J. M. *Trends Polym. Sci.* **1996**, *4*, 6.
- (11) Guenet, J. M.; McKenna, G. B. *Macromolecules* **1988**, *21*, 1752.
- (12) Spěváček, J.; Suchopárek, M. *Macromol. Symp.* **1997**, *114*, 23.
- (13) Kusuyama, H.; Miyamoto, N.; Chatani, Y.; Tadokoro, H. *Polym. Commun.* **1983**, *24*, 119.
- (14) Abe, H.; Imai, K.; Matsumoto M. *J. Polym. Sci. Part C* **1968**, *23*, 469.
- (15) Morris, G. A.; Freeman, R. *J. Magn. Reson.* **1978**, *29*, 433.
- (16) Spěváček, J.; Suchopárek, M. *Macromolecules* **1997**, *30*, 2178.
- (17) Saiani, A.; Guenet, J. M. *Macromolecules* **1997**, *30*, 966.
- (18) Reisman, A. In *Phase Equilibria*; Academic Press: New York, 1970.
- (19) Rundle, R. E.; Schull, C. G.; Wollan, E. O. *Acta Crystallogr.* **1952**, *5*, 22.
- (20) Point, J. J.; Damman, P.; Guenet, J. M. *Polym. Commun.* **1991**, *32*, 477.
- (21) Spěváček, J.; Schneider, B. *Makromol. Chem.* **1975**, *176*, 3409.
- (22) Valensin, G.; Kushnir, T.; Navon, G. *J. Magn. Reson.* **1982**, *46*, 23.
- (23) Spěváček, J.; Schneider, B. *Polym. Bull.* **1980**, *2*, 227.
- (24) Spěváček, J.; Schneider, B.; Straka, J. *Macromolecules* **1990**, *23*, 3042.

MA9710693